Nonequilibrium fission and heavy residue production in the interaction of 12–16 MeV/nucleon ^{32}S with ^{165}Ho

C. Casey, W. Loveland, and Z. Xu
Department of Chemistry, Oregon State University, Corvallis, Oregon 97331

L. Sihver and K. Aleklett
Studsvik Neutron Research Laboratory, S-611 82 Nyköping, Sweden

G. T. Seaborg
Nuclear Science Division, Lawrence Berkeley Laboratory, Berkeley, California 94720
(Received 12 September 1988; revised manuscript received 31 March 1989)

The target fragment production cross sections, angular distributions, and range distributions have been measured for the interaction of 12–16 MeV/nucleon ^{32}S with ^{165}Ho. The fragment isobaric yield distribution and the fragment moving frame angular distributions have been deduced from the data. Symmetry properties of the moving frame angular distributions have been used to establish a relative time scale for the reaction mechanism(s). No fission fragment moving frame angular distribution is symmetric about 90°, suggesting that these products are produced, in part, by a fast, nonequilibrium process. The range distributions are used to deduce energy spectra, which suggest that the heavy residues are the result of complete or incomplete fusion and also of an inelastic process such as deep inelastic scattering.

I. INTRODUCTION

Studies of intermediate energy nuclear collisions are thought to be interesting because of the "transitional" character of the intermediate energy regime. In low energy nuclear collisions, the behavior of the colliding nuclei is determined by their mean field. In high energy nuclear collisions, it is the collision of individual nucleons in the colliding nuclei that determines the outcome of the reaction. The intermediate energy regime (projectile energies of 10–100 MeV/nucleon) is thought to afford the opportunity of studying how nuclear reaction mechanisms change between these two extreme types of nuclear behavior.

The study of intermediate energy nuclear collisions has many aspects. In this discussion, we shall focus our attention on the experimental characterization of the fragments of the heavy target nucleus produced in such collisions. These fragments may be roughly classified by mass number, i.e., the intermediate mass fragments ($A_{\text{frag}} < A_{\text{target}}/3$), the heavy residues ($A_{\text{frag}} > \frac{2}{3} A_{\text{target}}$), and the fission fragments ($A_{\text{target}}/3 < A_{\text{frag}} < \frac{2}{3} A_{\text{target}}$). Interest in this area by experimentalists and theorists has been quite high, judging from the large number of survey papers and original contributions[1–30] that have appeared recently. From these many investigations, certain general features of the production of the target fragments have been discerned. They are the following.

(1) The heavy residue production cross sections represent a significant fraction of the total reaction cross section (Refs. 5, 7, 12, 23, 24, 27, and 29). The heavy residues are produced mostly in peripheral collisions at the higher projectile energies [35 and 44 MeV/nucleon (Refs. 18, 23, and 30)], although some residues at higher energies result from more central collisions as do most residues at lower projectile energies[23,30] where they can be characterized as evaporation residues.[27] The heavy residue angular distributions are strongly forward peaked in all cases.[23,24,27] Their velocities range from very low (at higher projectile energies where detector thresholds preclude observation of some residues[24,27]) to velocities exceeding that of the center of mass (indicating the existence of large nuclear excitation energies). Most of these fragments are produced in incomplete fusion reactions[11,12,18,23,30] although some are produced in nearly complete fusion events.[23,30]

(2) The intermediate mass fragment production cross sections are substantially lower than those of the heavy residues. They are predominantly produced with a multiplicity of unity in binary events that also yield a heavy residue.[3,14,17,25,26] The reactions producing them involve both nonequilibrated and equilibrated sources with the former being more important (in reactions induced by carbon projectiles).[17,31,32] Incomplete fusion with substantial preequilibrium particle emission is the dominant production mechanism.[14,17,26]

(3) The fission fragments represent those primary heavy residues that deexcited by fission rather than particle emission[12,24,27] and also can represent the result of a special nuclear reaction mechanism, fast fission.[3,6,10,28] In the former case, the ratio of the heavy residue to fission cross sections increases with increasing projectile energy due to two effects: (i) the increasing probability of incomplete fusion, leading to lower mass and atomic numbers of the product nuclei, this decreasing their fissionability, and (ii) the faster time scale of the more energetic reactions favors the intrinsically faster process of particle emission versus the slower collective motion of fission.[27]

Whether fission selects the high momentum transfer events relative to those of lower momentum transfer is a complicated feature of the deexcitation of a given set of nuclei.

Recently Aleklett *et al.*[33] have studied the interaction of 17 MeV/nucleon ^{32}S, 32 MeV/nucleon ^{40}Ar, and 44 MeV/nucleon ^{40}Ar with ^{197}Au. They observed a fast nonequilibrium fission process associated with central collision events in these reactions. This observation motivated the present study in that we wanted to further characterize this nonequilibrium fission process. To do so, we studied the interaction of 16 MeV/nucleon ^{32}S with a different nucleus, ^{165}Ho. By changing the target nucleus to ^{165}Ho, a nucleus that only fissions when made to rotate rapidly,[34] we hope to observe the effects of a higher fission barrier, higher angular momentum of the fissioning system, and a smaller change in deformation in going from saddle to scission upon this nonequilibrium fission mode. We were also aware of the existence of a large amount of data[35] for the interaction of intermediate energy, lighter projectiles, such as ^{12}C and ^{16}O, with ^{165}Ho.

II. EXPERIMENTAL PROCEDURES

Inclusive measurements of the target fragment yields, angular distributions, and differential range spectra for the interaction of 529 MeV ^{32}S with ^{165}Ho were made using radiochemical techniques. The accelerator used in the irradiations was the Lawrence Berkeley Laboratory (LBL) 88-inch cyclotron. The measurements were made using techniques that have been described previously.[31,32,36–38] Two irradiations, of duration 1.25 and 6.53 h, respectively, were performed to determine the target fragment yields (total fluences 2.4×10^{15} and 6.7×10^{16} ions, respectively). The targets for these irradiations were $\sim$90 mg/cm^2 thick, giving[39] a center-of-target energy of $\sim$380 MeV ($\sim$12 MeV/nucleon). Two irradiations were used for the angular and range distribution measurements of 16.2 and 14.2 h with particle fluences of 2.9×10^{15} and 5.4×10^{15} particles, respectively. Because of the thinner targets involved (152 μg/cm^2 Ho deposits on a 2.95 mg/cm^2 Be backing), the center-of-target energies were 508 MeV (16 MeV/nucleon).

The angular distributions were measured using the same techniques used for the 85 MeV/nucleon ^{12}C+^{197}Au, ^{238}U measurements.[31,32] Target fragments recoiling from the thin holmium deposits were stopped in a set of mylar catcher foils arranged in a cylindrical geometry. Following irradiation, the catcher foils were divided into ten pieces corresponding to the angular intervals 5.7–7.6°, 7.6–18.7°, 18.7–24.2°, 24.2–32.3°, 32.3–43.5°, 43.5–62.2°, 62.2–83.5°, 99.0–117.8°, 117.8–133.6°, and 133.6–158.2°. These pieces were assayed by gamma-ray spectroscopy beginning a few minutes after the end of irradiation and continuing for periods up to two months in laboratories at LBL and Oregon State University. After identifying the activities present in each foil and the amount of each radionuclide present, differential cross sections for each angular interval were calculated.

No correction was made for the finite angular resolution of the catcher foils because detailed numerical simulations[40] showed the effects were negligible. [The principal effect ($\sim$5%) is on the first angular interval (5.7–7.6°)]. The effects of nuclear stopping and straggling in the target upon the angular distributions were evaluated[40] in a manner similar to that used previously[31] with a similar conclusion. The conclusion is that stopping of the target fragments in the holmium deposit and large-angle scattering of the fragments from the beryllium target backing or the holmium target material is negligible. Small-angle scattering of the target fragments in the holmium target does occur and tends to "smear out" the measured distributions for the heavy residues. For the fission fragments, this effect is negligible.

For the range distribution measurements, all target fragments recoiling into the angular interval from 9.1 to 21.8° were stopped in a stack of eleven mylar foils ranging in thickness from 0.29–10.7 mg/cm^2. The cumulative stack thickness was 41.7 mg/cm^2. The stack consisted of three foils that were $\sim$0.3 mg/cm^2, three foils that were $\sim$0.9 mg/cm^2, two foils of thickness $\sim$3.3 mg/cm^2, and three foils that were $\sim$10.6 mg/cm^2 thick. Following irradiation, each foil was assayed by gamma-ray spectroscopy.

Two effects contribute to the resolution obtained in the measured range distributions: the finite, unequal thicknesses of the catcher foils used and the range straggling inherent in the stopping process. (We neglect straggling due to catcher foil inhomogeneities and different path lengths in the target. Numerical simulations show that the straggling introduced by the finite solid angle subtended by the cather foils is negligible.) Numerical simulations using the LSS stopping power theory[41] and the approach of Hvelplund[42] give a range straggling of $(\Delta v^2/v^2)\sim0.1$, where v is the velocity of an 8.4-MeV ^{167}Tm fragment stopping in mylar. (The straggling for fission fragments is $\sim\frac{1}{3}$ of this.) Thus some broadening of the heavy residue spectra is expected, but should not change the qualitative observations.

III. RESULTS

For the reaction of 12–16 MeV ^{32}S with ^{165}Ho, partial and complete angular distributions of eight different target fragments were measured along with the production cross sections for 75 different radionuclides. Differential range distributions were obtained for 31 radionuclides.

A. Target fragment yields

The measured target fragment production cross sections are shown in Table I. We have taken a conservative approach in this tabulation and have eliminated from the table all nuclides whose atomic and mass numbers are such that they could possibly be degraded projectile fragments. In doing so, we have effectively eliminated intermediate mass fragments from our study. We have deduced mass yield (isobaric yield) distributions from the measured formation cross sections. The method employed in this estimation procedure has been discussed

TABLE I. Formation cross sections (mb) of nuclides formed by the reaction of 12 MeV/nucleon ^{32}S with ^{165}Ho. Independent yields are indicated by (*I*). By the term "independent yield" we refer to the yields of shielded nuclides, quasishielded nuclides, and nuclides whose production by precursor decay is not significant.

Nuclide	Cross section	Nuclide	Cross section
^{42}K	9.8±0.5	$^{101}Rh^m$	33±1.0
^{43}K	11.2±0.3	^{105}Ag	33±5
^{46}Sc (*I*)	11.5±0.5	^{111}In	30.6±0.7
^{47}Ca	1.60±0.06	^{123}I	36±1
^{48}Sc (*I*)	5.2±0.6	^{123}Xe	15.9±0.8
^{48}V	2.26±0.03	^{124}I	3.8±0.2
^{52}Mn	1.50±0.01	^{126}Ba	7.7±0.9
^{56}Mn	18±2	^{127}Cs	14.3±0.54
^{59}Fe	10.0±0.3	^{127}Xe	15±6
^{65}Zn	15±1	^{128}Ba	25±8
^{69}Ge	11.2±0.9	^{129}Cs	20.2±0.8
^{73}Se	4.2±0.1	^{132}Ce	10.0±0.6
^{74}As	30±2	^{135}Ce	16±2
^{75}Se	29.4±0.9	^{139}Ce	6±1
^{75}Br	2.5±0.2	^{145}Eu	11.2±0.3
^{76}Br	14±6	^{146}Eu	7.4±0.4
^{77}Br	32±2	^{149}Gd	24±1
^{79}Kr	21±10	^{151}Tb	18±3
^{81}Rb	18.1±0.9	^{152}Tb	15±2
^{82}Br (*I*)	5.8±0.4	^{153}Tb	27±2
$^{82}Rb^m$	28±4	^{155}Tb	37±11
^{83}Rb	56±4	^{155}Dy	31.3±0.7
^{84}Rb (*I*)	39±1	^{156}Tb (*I*)	5.5±0.2
^{86}Y	28±2	^{157}Dy	48.7±0.9
^{87}Y	62.3±0.9	^{160}Er	94±6
^{88}Y	40±2	^{161}Er	82±3
^{88}Zr	36±2	^{163}Tm	94±22
^{89}Zr	51±1	^{165}Tm	156±23
^{90}Nb	25±2	^{166}Yb	54±5
$^{92}Nb^m$ (*I*)	1.6±0.5	^{167}Tm	76±4
^{93}Tc	3.3±0.3	^{169}Lu	29±1
^{94}Tc	10±2	^{170}Hf	16.9±0.8
^{95}Ru	3.1±0.2	^{171}Hf	14±1
^{95}Tc	18±3	^{173}Hf	12.7±0.4
^{96}Tc (*I*)	30.6±0.2	^{173}Ta	4±2
^{97}Ru	18.1±0.7	^{175}Hf	22±1
^{100}Rh	23.6±0.4		

previously.[36]

The measured nuclidic formation cross sections were placed in eight groups according to mass number. These cross sections were corrected for precursor beta decay, where necessary, by assuming that the independent yield cross sections for a given species, $\sigma(Z,A)$, can be expressed as a histogram that lies along a Gaussian curve:

$$\sigma(Z,A)=\sigma(A)[\pi C_Z^2(A)]^{-1/2} \times \exp[-(Z-Z_{mp})^2/2C_Z^2(A)] , \quad (1)$$

where $C_Z(A)$ is the Gaussian width parameter for mass number A and $Z_{mp}(A)$ is the most probable atomic number for that A. Using this assumption and the further assumption that $\sigma(A)$ varies slowly and smoothly as a function of A [allowing data from adjacent isobars to be combined in determining $Z_{mp}(A)$ and $C_Z(A)$], one can use the laws of radioactive decay to correct iteratively the measured cumulative formation cross sections for precursor decay.

Within each of the eight groups, the data were fit to a Gaussian-shaped independent-yield distribution. The width parameter was found to be constant over a given range in A. The centers of the charge distributions were

TABLE II. Charge dispersion parameters.

Fragment Mass number range	$Z_{mp}(A)$	$C_Z(A)$
42–49	$0.433A+1.07$	0.7
65–79	$0.438A+0.76$	0.7
81–89	$0.441A+0.37$	0.7
90–100	$0.439A+0.70$	0.8
101–124	$0.384A-6.20$	0.9
126–139	$0.373A-7.85$	0.9
145–160	$0.375A-7.63$	0.7
161–175	$0.362A+9.76$	0.3

adequately represented by linear functions in A over a limited range in A although we expect $Z_{mp}(A)$ to be nonlinear. (Only nuclides with well-characterized beta-decay precursors and cases where both members of an isometric pair were observed were included in the analysis.) The nuclidic groupings along with the centers and widths of the Gaussian distributions are given in Table II. The independent-yield distributions estimated from the measured formation cross sections are shown in Fig. 1.

The isobaric yield distribution obtained from integration of the estimated independent yield distributions is shown in Fig. 2. The error bars on the integrated data

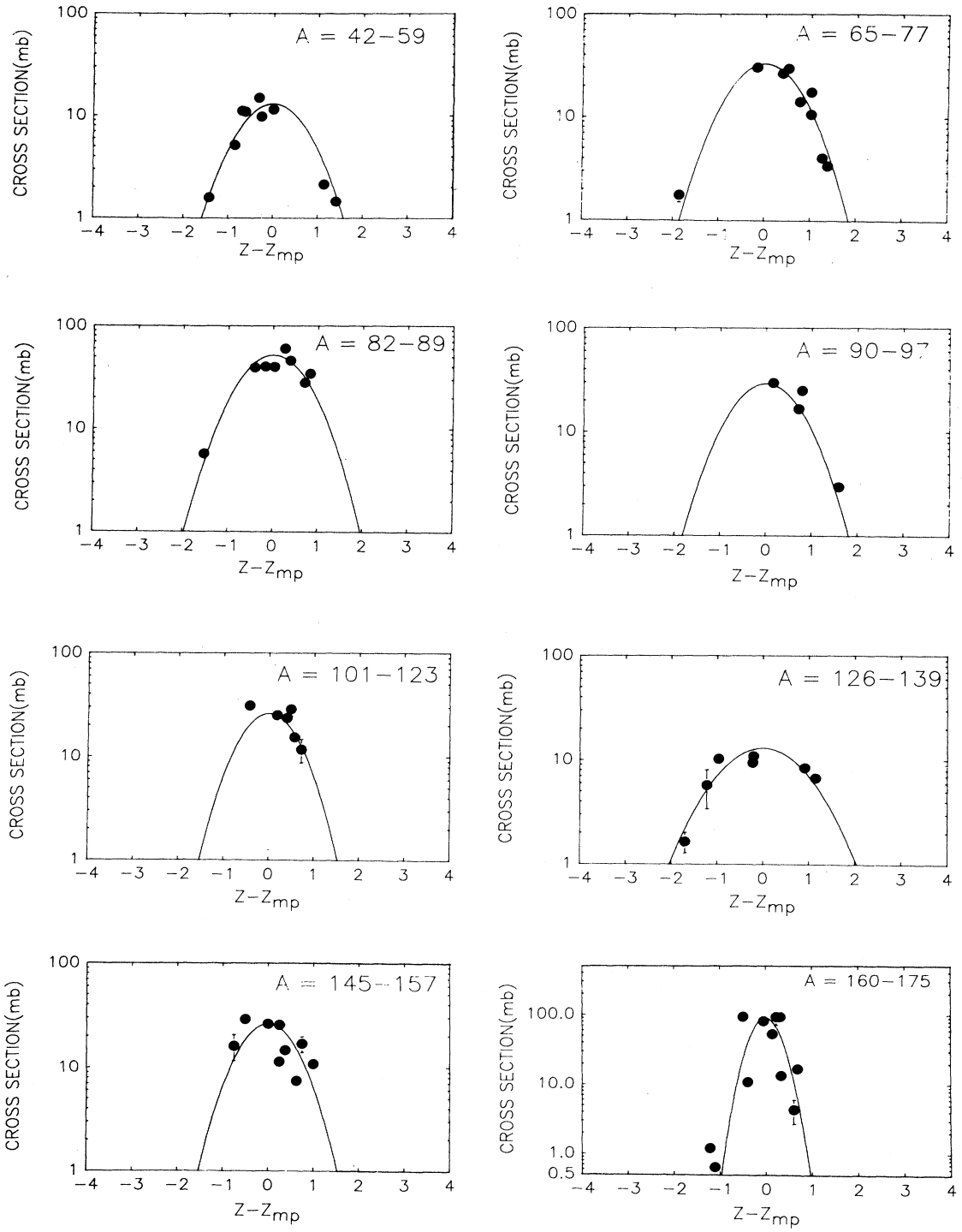

FIG. 1. The independent yield distributions from the reaction of 12 MeV/nucleon ^{32}S with ^{165}Ho. The plotted points are the independent yield cross sections calculated from the data while the solid lines are the Gaussian charge dispersions used in the calculation.

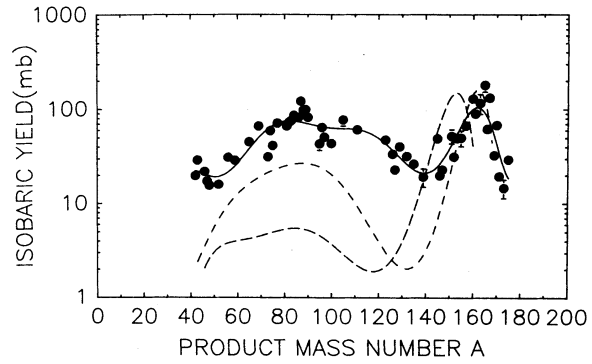

FIG. 2. Isobaric yield distributions for the fragmentation of ^{165}Ho by (a) 12 MeV/nucleon ^{32}S, solid points, solid line; (b) 17 MeV/nucleon ^{16}O (Ref. 35), short-dashed line; (c) 442 MeV ^{12}C (Ref. 35), long-dashed line.

points reflect the uncertainties due to counting statistics and those introduced in the charge distribution fitting process. Morrissey *et al.*[36] have suggested that individual isobaric yields may have systematic uncertainties, due to the fitting process, of approximately 25%. Uncertainties due to lack of knowledge of the absolute beam intensity (estimated to be approximately 15%), and contributions due to secondary reactions (possibly as large as 10%) have been neglected. Also shown as smooth curves in Fig. 2 are the isobaric yield distributions for the interaction[35] of roughly equivalent velocity ^{16}O ions with ^{165}Ho (normalized to the ^{32}S+^{165}Ho total reaction cross section[43]) as well as roughly equivalent total projectile energy ^{12}C with ^{165}Ho. One notes two prominent peaks in the isobaric distributions, a fission peak ($A=50-146$) and a heavy residue peak ($A>146$). The fission cross section is enhanced for the ^{32}S+^{165}Ho reaction relative to the other reactions ($\sigma_f=2060$ mb) with especially higher yields of the heavy mass fission products. The latter observation is consistent with the larger A value of the completely fused system in the ^{32}S+^{165}Ho reaction.

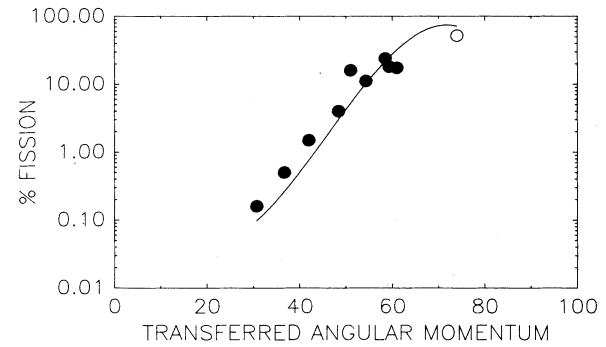

FIG. 3. Empirical systematics relating the fission probability to a semiclassical measure of the transferred angular momentum in the reaction.[34] The solid points refer to the interaction of ^{12}C and ^{16}O with ^{165}Ho, the open point refers to ^{32}S+^{165}Ho (this work), and the solid line represents the result of a calculation using a statistical model for the deexcitation of hot, rotating nuclei.

The relative fission cross section in these reactions can be understood in terms of a correlation[34] between the relative fission cross section and the angular momentum transferred to the target nucleus (Fig. 3). The data from the ^{32}S+^{165}Ho appear to fit well into the previously established correlation.

B. Target fragment angular distributions

Full or partial angular distributions for 82 different target fragments were measured. A representative set of these distributions is shown in Fig. 4. The laboratory frame angular distributions are all strongly forward peaked. The heavy residue distributions ($A>146$) have different shapes than those associated with the fission products. This is consistent with relative momentum kicks given the primary fragments by fission or sequential particle emission.

Each fragment angular distribution was integrated from 0 to $\pi/2$ and from $\pi/2$ to π to obtain the ratio of fragments recoiling forward (F) from the target to those recoiling backward (B). To extract further information from the data, the laboratory system angular distributions were transferred into the moving frame (MF) of the target residue following the initial target-projectile encounter. To do this, we have assumed that the final velocity of the fragment in the laboratory system can be written as $V_{\rm lab}=V+v$, where the velocity v is the velocity of the moving frame and V is the velocity kick given the target fragment by particle emission or fission at an angle $\theta_{\rm MF}$ with respect to the beam direction in the moving frame. The vector v has components of v_{11} and v_t, parallel and perpendicular to the beam direction. In lieu of detailed information about v_t, the forward-peaked nature of the distributions, and the difficulty of obtaining information about v_t, we have assumed $v_t=0$. We have used standard formulas[44] to make laboratory frame transformations for $d\sigma/d\Omega$ and θ.

For the value of $\eta_{11}(=v_{11}/V)$ needed to make such transformations, we have used η_{11} as derived from integrating the angular distributions. To get the value of η_{11} from F and B, we assume the angular distribution of the fission fragments in the moving frame can be represented as $1+\alpha\cos^2\theta_{\rm MF}$. In this case, it can be shown[45] that

$$F=\tfrac{1}{2}[1+(1+\eta^2\alpha/3)\eta/(1+\alpha/3)]\ ,$$

$$B=\tfrac{1}{2}[1-(1+\eta^2\alpha/3)\eta/(1+\alpha/3)]\ .$$

These equations were solved by finding the value of η that minimized $(F/B)_{\rm MF}$. Previous work[33] has shown that values of η_{11} deduced in this manner agree with directly measured values. A representative set of the resulting moving frame angular distributions for the fission fragments is shown in Fig. 5. (Not enough data was available at backward angles to meaningfully transform the heavy residue distributions.) None of the moving frame angular distributions is symmetric about 90° in the moving frame (Fig. 6).

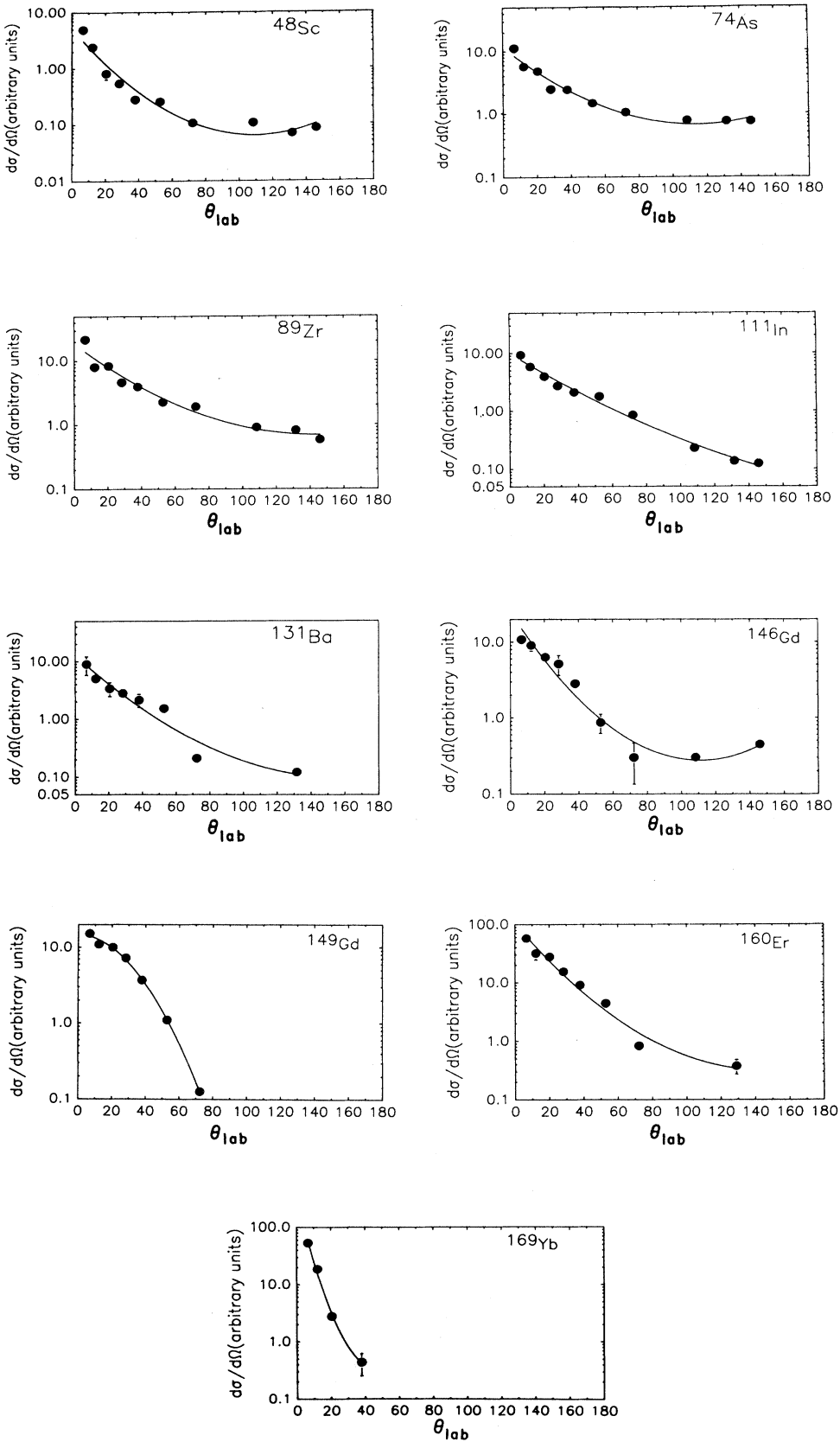

FIG. 4. Representative laboratory frame fragment angular distributions for the interaction of 16 MeV/nucleon ^{32}S with ^{165}Ho.

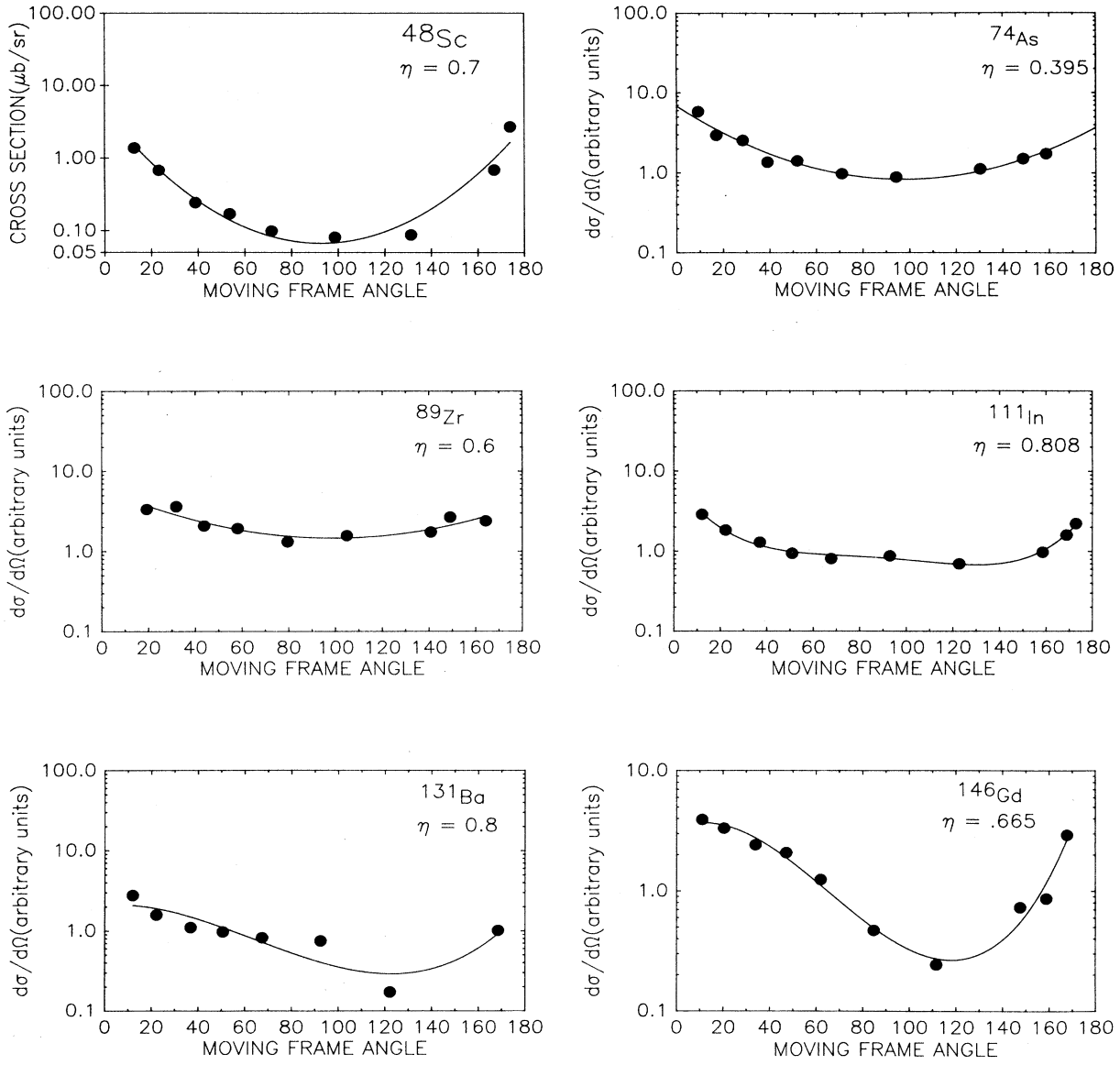

FIG. 5. Moving frame angular distributions derived from the data of Fig. 4.

What is the meaning of this lack of symmetry? The use of η_{11} derived in this manner tacitly assumes the moving frame distribution is symmetric about 90° but allows for an anisotropy in the moving frame.[45] The failure to observe a symmetric moving frame distribution implies an improper transformation, but the fact that for certain nuclides no value of η_{11} will lead to a symmetric distribution (Fig. 5) implies a more fundamental problem. We believe that this unique observation suggests the occurrence of a fast, nonequilibrium mode of fission (similar to that previously observed[33] for the reaction of 17–44 MeV/nucleon ^{32}S and ^{40}Ar with ^{197}Au.) However, unlike the ^{32}S, ^{40}Ar+^{197}Au reactions where this mechanism was only discernible in the angular distribution of the heavy mass fission fragments, the occurrence of this mechanism is clearly seen for all fission fragments although it is most

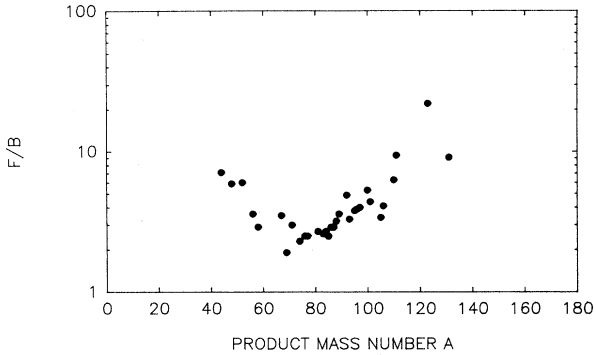

FIG. 6. The forward-to-backward ratios (F/B) vs product mass number for the moving frame distributions shown in Fig. 5.

prevalent for the high mass number fragments (Fig. 6). We should remember that the use of the same procedure to treat the data in the 17–44 MeV/nucleon ^{32}S, $^{40}Ar+^{197}Au$ reaction led to symmetric moving frame distributions for most fission fragments. Furthermore, the observation of asymmetric moving frame distributions does not mean all fission events are "fast." The observation implies only that a large enough fraction of the fission events needed to cause asymmetric distributions occurs.

C. Target fragment energy spectra

The measured differential range spectra were converted to energy spectra using standard range-energy tables.[46] A representative set of these data is shown (in Fig. 7). The energies of the fission fragments are consistent with what is expected for the fission of composite nuclei following the complete fusion of 16 MeV/nucleon ^{32}S with ^{165}Ho. The ^{160}Er spectrum is typical of those spectra for fragments with $A=140-165$, showing peaks in the energy spectra at 0.1 MeV/nucleon and 0.5 MeV/nucleon.

IV. DISCUSSION OF RESULTS

A. Heavy residues

At projectile energies of 12–16 MeV/nucleon, one would expect that about 15–25 % of the reactions involved complete fusion.[43] The success of the Boltzmann master equation model of Blann[47] in accounting for many features of intermediate energy heavy ion reactions would suggest that a large fraction of the reactions would involve preequilibrium emission. We have used the computer program LINDA (Ref. 48) to simulate the production of the heavy residues assuming production via (a)

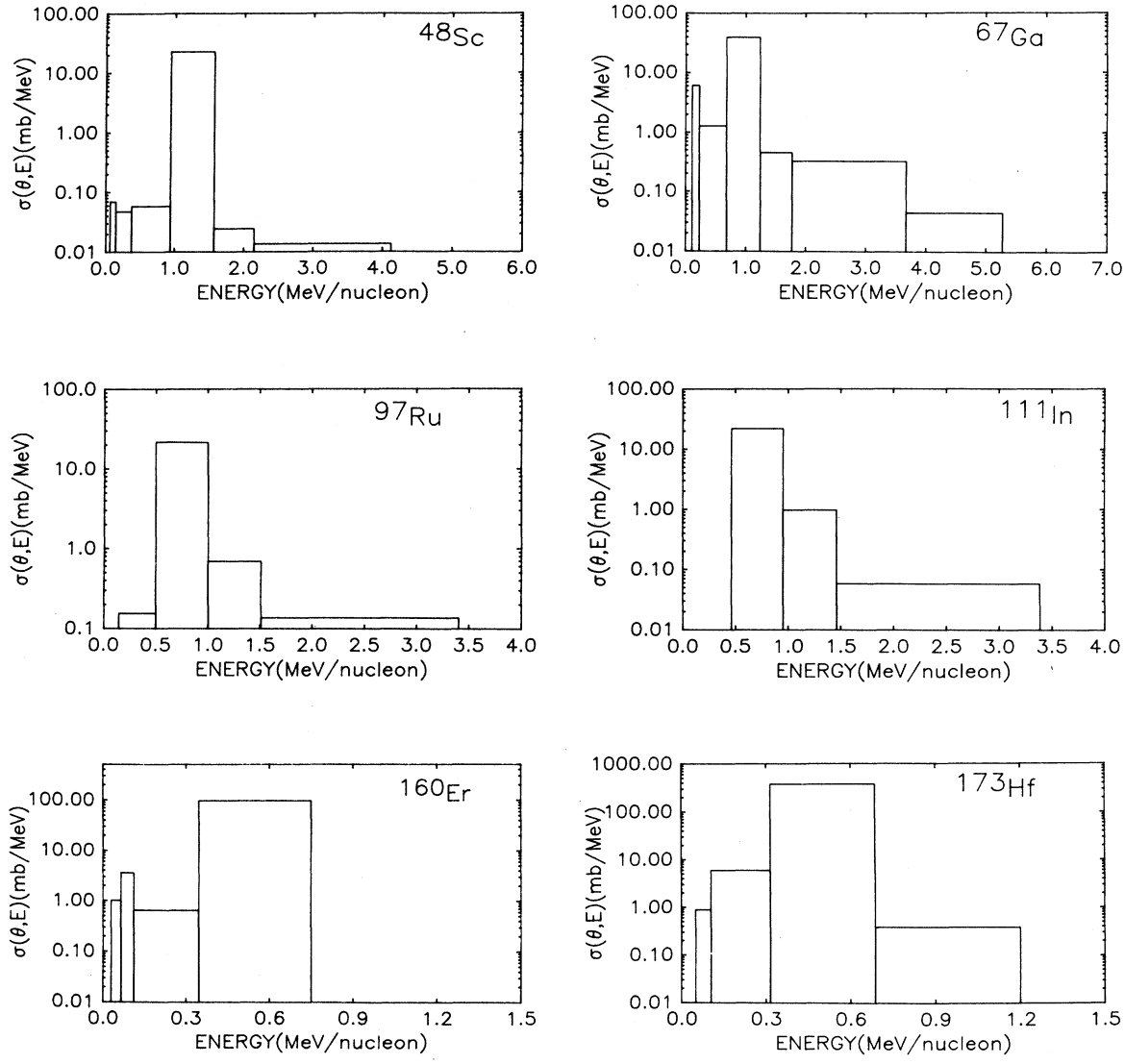

FIG. 7. Representative fragment energy spectra for the interaction of 16 MeV/nucleon ^{32}S with ^{165}Ho.

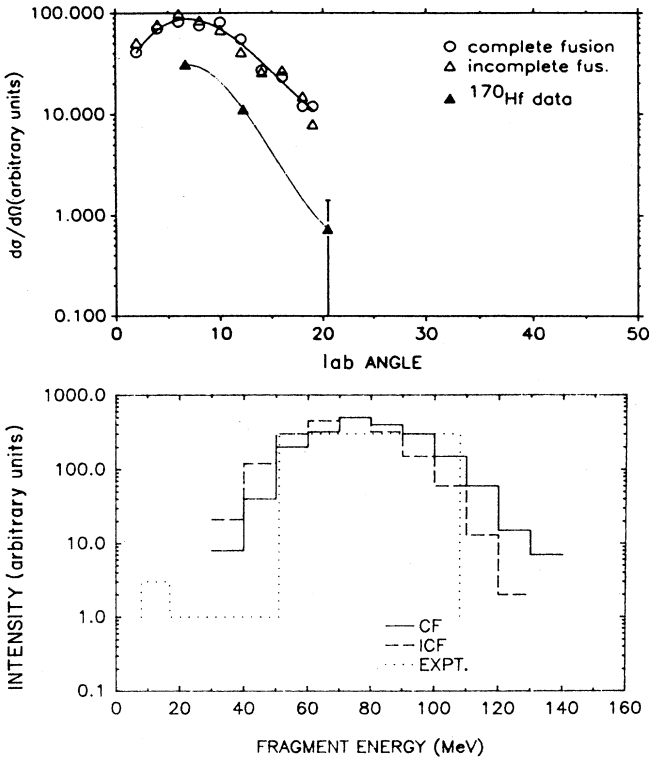

FIG. 8. Comparison of the predicted heavy residue angular distributions and energy spectra for an $A=170$ fragment with the observed ^{170}Hf data.

complete fusion or (b) preequilibrium emission as predicted by the Blann preequilibrium emission model. (For this reaction, two protons and five neutrons were predicted to be emitted before establishing equilibrium.)

The results of the simulations are compared to the experimental data for a typical heavy residue, ^{170}Hf, in Fig. 8. The predicted differences between the two reaction mechanisms are barely discernible. The resolution of the measured data does not allow one to determine which mechanism is dominant but the data agrees well with their prediction.

As noted previously, in addition to the main peak in the heavy residue energy spectra at ~0.5 MeV/nucleon due to complete or incomplete fusion, there is another peak at ~0.09 MeV/nucleon. Such energies are consistent with the production of these fragments in deep inelastic events where $Q\sim-200$ MeV. The resulting damped projectilelike fragments ($A\sim30$) would have energies ~10–11 MeV/nucleon, which is consistent with the range spectra of fragments such as ^{28}Mg.

B. Fission products

None of the fission products had moving frame angular distributions which were symmetric about 90°. This fact suggests the production, in part, of these fragments by a fast, nonequilibrium mechanism. Production of these fragments by a normal, "slow" fission process would be expected to occur also. A modest contribution of nonequilibrium fission events to the total fission fragment angular distributions would cause them to be asymmetric. (In this context, "slow" and "fast" are defined relative to the time estimated[49] for establishing statistical equilibrium in an excited nuclear system of $2-3\times10^{-23}$ sec).

A known nuclear reaction mechanism for low energy nucleus-nucleus collisions, "fast fission" or "quasifission" (Ref. 28) is a possible candidate for the suggested nonequilibrium mechanism. In this mechanism, all partial waves between the l wave at which the fission barrier vanishes, $l_{B_f}=0$, and the critical angular momentum, $l_{\rm crit}$, go via fast fission. In these events, the fusing system never reaches a configuration inside the fission saddle point and the resulting fission event is fast. Experimental signatures for such events are the lack of symmetry of the angular distributions in the moving frame and a broader than normal fission mass distribution (Fig. 2). Unlike the previous studies[33] of the intermediate energy ^{32}S, ^{40}Ar+^{197}Au reactions where it was possible to resolve the fragment angular distributions into "slow" and "fast" components, the lack of any distribution being symmetric in the moving frame precludes such a decomposition. As a first guess at an alternate decomposition, if one assumes the slow equilibrium component of the fission cross section to be ~1620 mb (as observed in the 17 MeV/nucleon ^{16}O+^{165}Ho reaction where $l_{B_f=0}>l_{\rm crit}$), then one obtains by difference, an estimated nonequilibrium cross section of 440 mb, which is twice the expected fast fission cross section. A similar effect was observed by Aleklett *et al.*[33] for the reaction of 17 A MeV ^{32}S with ^{197}Au, where the nonequilibrium fission cross section was estimated to be 2.9 times the fast fission cross section.

The measured fission cross section for the 12 MeV/nucleon ^{32}S+^{165}Ho reaction seems to fit in well with a previously established empirical correlation[34] between the fraction of primary residues that fission and a semiclassical estimate of the angular momentum transferred to the target nucleus. We attempted to see if this apparent empirical correlation observed for the interaction of ^{12}C, ^{16}O, and ^{32}S nuclei with ^{165}Ho would be expected from standard statistical-model calculations of the deexcitation of highly excited nuclei. As our "standard statistical model" we used the PACE code,[50] an angular momentum dependent Monte Carlo model. For projectile energies below 10 MeV/nucleon, we simply treated the problem as a compound nucleus formation and decay problem. The fusion cross sections were adjusted to published systematics of experimental data.[43] The ratio of level density parameters a_f/a_n was taken to be 1.000. The finite-range rotating liquid drop fusion barriers of Sierk[51] were used in the calculation. For projectile energies above 10 MeV/nucleon, the distribution of (E^*,J,Z,A) of the target fragments following the primary nucleus-nucleus collision was calculated using the Boltzmann master equation model as described previously.[52] The results of these simulations are shown in Fig. 3. Although there are some differences between the calculated and measured fission probabilities in each system, the calculations generally reproduce the data. While the fission probabilities shown in Fig. 3 reflect both the

effects of E^* and J of the fissioning system, the primary effect (in the statistical model) is one due to the J of the fissioning system.

V. CONCLUSIONS

What new information have we gained about intermediate energy nucleus-nucleus collisions from this study? The use of radiochemical techniques for measuring energy spectra and the use of very thin targets has allowed us to measure the heavy residue energy spectra down to very low energies. These measurements seem to indicate the occurrence of deep inelastic scattering as a heavy residue production mechanism (in the interaction of 16 MeV/nucleon ^{32}S with ^{165}Ho).

The fission fragment mass distribution observed in this work is substantially broader than that observed in the interaction of equivalent velocity or total projectile kinetic energy ^{12}C and ^{16}O projectiles with ^{165}Ho. The angular distributions show the importance of fast, nonequilibrium fission processes. The relative dominance of these processes when ^{165}Ho is the target nucleus compared to ^{197}Au could be due to the larger fraction of fission events taking place at high angular momentum. The previously established empirical correlation between fission probability and the semiclassical measure of the transferred angular momentum in the reaction has been shown to be consistent with a standard statistical model for the deexcitation of hot rotating nuclei.

ACKNOWLEDGMENTS

We wish to thank Ruth Mary Larimer and the crew of the 88-inch cyclotron for their help as well as Diana Lee of the Lawrence Berkeley Laboratory (LBL) for assistance during counting of samples. Helpful discussions with T. T. Sugihara are gratefully acknowledged. This work was supported in part by the U.S. Department of Energy through Grant No. DE-FG06-88ER40402.

[1]S. Levit, in *Proceedings of the International Nuclear Physics Conference, Harrogate, 1986,* edited by J. L. Durell, J. M. Irvine, and G. C. Morrison (Institute of Physics, Bristol, 1987), p. 227.

[2]M. Conjeaud, S. Harar, M. Mostefai, E. C. Pllaco, C. Volant, Y. Cassagnou, R. Dayras, R. Legrain, H. Oeschler, and F. Saint-Laurent, Phys. Lett. **159B**, 244 (1985).

[3]S. Harar, Nucl. Phys. **A471**, 205C (1987).

[4]B. Tamain, in *Proceedings of the International Nuclear Physics Conference, Harrogate, 1986,* edited by J. L. Durell, J. M. Irvine, and G. C. Morrison (Institute of Physics, Bristol, 1987), p. 247.

[5]F. Hubert, R. Del Moral, J. P. Dufour, H. Emmermann, A. Fleury, C. Poinot, M. S. Pravikoff, H. Delegrange, and A. Lleres, Nucl. Phys. **A456**, 535 (1986).

[6]H. Delagrange, C. Gregoire, Y. Abe, and N. Carjan, J. Phys. (Paris) **47**, 305 (1986).

[7]J. Blachot, J. Crancon, B. deGoncourt, A. Gizon, and A. Lleres, Z. Phys. **A321**, 645 (1985).

[8]H. Nifenecker, J. Blachot, J. Crancon, A. Gizon, and A. Lleres, Nucl. Phys. **A447**, 533C (1985).

[9]D. Jacquet, E. Duek, J. M. Alexander, B. Borderie, J. Galin, D. Gardes, D. Guerreau, M. Lefort, F. Monnet, M. F. Rivet, and X. Tarrago, Phys. Rev. Lett. **53**, 2226 (1984).

[10]W. P. Zank. D. Hilscher, G. Ingold, U. Jahnke, M. Lehmann, and H. Rossner, Phys. Rev. C **33**, 519 (1986).

[11]D. Guerreau, Nucl. Phys. **A447**, 37C (1985).

[12]C. Cerruti, D. Guinet, S. Chiodelli, A. Demeyer, K. Zaid, S. Leray, P. Lhenoret, C. Mazur, C. Ngo, M. Ribrag, and A. Lleres, Nucl. Phys. **A453**, 175 (1986).

[13]Y. Patin, S. Leray, E. Tomasi, O. Granier, C. Cerruti, J. L. Charvet, S. Chiodelli, A. Demeyer, D. Guinet, C. Humeau, P. Lheoret, J. P. Lochard, R. Lucas, C. Mazur, M. Morjean, C. Ngo, A. Pehaire, M. Ribrag, L. Sinopoli, T. Suomijarvi, J. Uzureau, and L. Vagneron, Nucl. Phys. **A457**, 146 (1986).

[14]K. Kwiatkowski, Nucl. Phys. **A471**, 271C (1987).

[15]See, for example, J. Pochodzalla, Nucl. Phys. **A471**, 289C (1987); W. G. Lynch, *ibid.* **A471**, 309C; D. Gross and H. Massmann, *ibid.* **A471**, 339C; J. P. Bondorf *et al.*, *ibid.* **A444**, 460 (1985).

[16]C. Gregoire, D. Jacquet, M. Pi. B. Remaud, F. Sebille, E. Suraud, P. Shuck, and L. Vinet, Nucl. Phys. **A471**, 399C (1987).

[17]V. E. Viola, Nucl. Phys. **A471**, 53C (1987).

[18]H. Delagrange and J. Peter, Nucl. Phys. **A471**, 111c (1987).

[19]D. Fabris, K. Hagel, J. B. Natowitz, G. Nebbia, R. Wada, R. Billerey, B. Cheynis, A. Demeyer, D. Drain, D. Guinet, C. Pastor, L. Vagneron, T. Zaid, J. Alarga, A. Giorni, D. Heuer, C. Morand, B. Viano, C. Mazur, C. Ngo, S. Leray, R. Lucas, M. Ribrag, and E. Tomasi, Nucl. Phys. **A471**, 351C (1987).

[20]G. Auger, E. Plagno, D. Jouan, C. Guet, D. Heuer, M. Maurel, H. Nifenecker, C. Ristori, F. Schussler, H. Doubre, and C. Gregoire, Phys. Lett. **169B**, 161 (1986).

[21]S. Leray, J. Phys. (Paris) Colloq. **47**, C4-273 (1986).

[22]A. Lleres, C. Guet, D. Heuer, M. Maurel, C. Ristori, F. Schussler, M. W. Curtain, and D. K. Scott, Phys. Lett. B **185**, 336 (1987).

[23]G. Bizard, R. Brou, H. Doubre, A. Drouet, F. Guilbualt, F. Hanappe, J. M. Harasse, J. L. Laville, C. Lebrun, A. Oubahadou, J. P. Patry, J. Peter, G. Ployart, J. C. Steckmayer, and B. Tamain, Z. Phys. A **323**, 459 (1986).

[24]G. Bizard, R. Brou, H. Doubre, A. Drouet, F. Guilbault, F. Hannappe, J. M. Harasse, J. Laville, C. Lebrun, A. Oubahadou, J. P. Patry, J. Peter, G. Ployart, J. C. Steckmayer, and B. Tamain, Nucl. Phys. **A456**, 173 (1986).

[25]B. Borderie, C. Cabot, H. Fuchs, D. Gardes, H. Gauvin, F. Hannappe, D. Jacquet, D. Jouan, F. Monnet, M. Montoya, and M. F. Rivet, Grand Accélérateur National d'Ions Lourds Report No. 22, 1987.

[26]D. J. Fields, W. G. Lynch, T. K. Nayak, M. B. Tsang, C. B. Chitwood, C. K. Gelbke, R. Morse, J. Wilczynski, T. C. Awes, R. L. Ferguson, F. Plasin, F. E. Obenshain, and G. R. Young, Phys. Rev. C **34**, 536 (1986).

[27]M. F. Rivet, B. Borderie, H. Gauvin, D. Gardes, C. Cabot, F. Hannappe, and J. Peters, Phys. Rev. C **34**, 1282 (1986).

[28]C. Gregoire, C. Ngo, and B. Remaud, Nucl. Phys. **A383**, 392 (1982).

[29]E. C. Pollacco, M. Conjeaud, S. Harar, C. Volant, Y. Cassagnou, R. Dayras, R. Legrain, M. S. Nguyen, H. Oeschler, and F. Saint-Laurent, Phys. Lett. **146B**, 29 (1984).

[30]Y. Patin *et al.*, Nucl. Phys. **A457**, 146 (1986).
[31]R. H. Kraus, Jr., W. Loveland, K. Aleklett, P. L. McGaughey, T. T. Sugihara, G. T. Seaborg, T. Lund, Y. Morita, E. Hagebo, and I. R. Haldersen, Nucl. Phys. **A432**, 525 (1985).
[32]K. Aleklett, W. Loveland, T. Lund, P. L. McGaughey, Y. Morita, G. T. Seaborg, and E. Hagebo, and I. Haldorsen, Phys. Rev. C **33**, 885 (1986).
[33]K. Aleklett, W. Loveland, L. Sihver, Z. Xu, C. Casey, D. J. Morrissey, J. O. Liljenzin, M. de Saint-Simon, and G. T. Seaborg, submitted to Nucl. Phys.
[34]W. Loveland, K. Aleklett, and G. T. Seaborg, Nucl. Phys. **A447**, 101C (1985).
[35]R. Kraus, Ph.D. thesis, Oregon State University, 1986 (unpublished).
[36]D. J. Morrissey, W. Loveland, M. de Saint-Simon, and G. T. Seaborg, Phys. Rev. C **21**, 1783 (1980).
[37]D. J. Morrissey, D. Lee, R. J. Otto, and G. T. Seaborg, Nucl. Instrum. Methods **158**, 499 (1978).
[38]K. Aleklett, M. Johanssen, L. Sihver, W. Loveland, H. Groening, P. L. McGaughey, and G. T. Seaborg, Nucl. Phys. (to be published).
[39]F. Hubert, A. Fleury, R. Bimbot, and D. Gardes, Ann. Phys. (Paris) **5**, 3 (1980).
[40]C. Casey, M.S. thesis, Oregon State University, 1988 (unpublished).
[41]J. Lindhard, M. Scharff, and H. Schiott, Mat. Fys. Medd. Dan. Vid. Selsk. **33**, No. 14 (1963).
[42]P. Hvelplund, Mat. Fys. Medd. Dan. Vid. Selsk. **38**, No. 4 (1971).
[43]W. W. Wilcke, J. R. Birkelund, H. J. Wollersheim, A. D. Hoover, J. R. Huizenga, W. U. Schroder, and L. E. Tubbs, At. Data Nucl. Data Tables **25**, 391 (1980).
[44]J. B. Marion, T. I. Arnette, and H. C. Owens, Oak Ridge National Laboratory Report ORNL-2574, 1959.
[45]J. M. Alexander, in *Nuclear Chemistry,* edited by L. Yaffe (Academic, New York, 1968), Vol. 1, pp. 273–357.
[46]L. G. Northcliffe and R. S. Schilling, Nucl. Data Tables **7**, 233 (1970).
[47]M. Blann, Phys. Rev. C **31**, 1245 (1985).
[48]E. Duek, L. Kowalski, and J. M. Alexander, Comput. Phys. Commun. **34**, 395 (1985).
[49]G. D. Harp, J. M. Miller, and B. J. Berne, Phys. Rev. **165**, 1166 (1968).
[50]A. Gavron, Phys. Rev. C **21**, 230 (1980).
[51]A. J. Sierk, Phys. Rev. C **33**, 2039 (1986).
[52]A. N. Behkami, W. Loveland, K. Aleklett, and G. T. Seaborg, in *Nuclear Fission and Heavy-Ion-Induced-Reactions,* edited by W. U. Schröder (Harwood, London, 1987), pp. 443–451.